



Semnan University



Research Article

Experimental Heat Transfer Analysis of Helical Coiled Tubes on the Basis of Variation in Curvature Ratio and Geometry

Susheel Madhavrao Magar ^{a*}, Gaurav Kumar Gugliani ^a, Ravindra Rambhau Navthar ^b

^a Department of Mechanical Engineering, Mandsaur University, Rewas Dewda Road, SH - 31, Mandsaur, Madhya Pradesh, 458001, India

^b Department of Mechanical Engineering, Dr. Vithalrao Vikhe Patil College of Engineering, Vadgaon Gupta, Ahmednagar, Maharashtra, 414111, India

ARTICLE INFO

Article history:

Received: 2023-10-28

Revised: 2024-03-24

Accepted: 2024-03-31

Keywords:

Curvature ratio;

Dean number;

Effectiveness;

Helical Cone Coil(HCC);

Pressure drop.

ABSTRACT

The influence of curvature ratio (CR) within helical tubes on secondary flows and subsequent enhancement of heat transfer is well-established. Furthermore, the interaction between the shell fluid and the helical tube is recognized as pivotal in this regard. In this paper, the impact of varying CR and coil geometry on the performance of heat exchangers (HEs) through experimental heat transfer analysis conducted on five distinct coils viz., straight helical ($\Theta = 90^\circ$), conical ($\Theta = 70^\circ, 50^\circ, 30^\circ$), and spiral ($\Theta = 0^\circ$) configurations have been studied. Moreover, correlations for modified effectiveness are proposed for all HEs. The Reynolds number range chosen for the analysis spans from 3700 to 20000, encompassing laminar and turbulent flow regimes of the coil hot water. The optimal HE is identified based on thermal and hydrodynamic parameters, including hot water temperature difference, effectiveness, modified effectiveness, rate of heat transfer, pressure drops of the coil, shell fluids, and pumping power. Observations reveal that helical cone coil heat exchangers (HCCHEs) demonstrate superior thermal and hydrodynamic characteristics when the fluid flow aligns with increasing CR. Notably, for both laminar and turbulent flows, the highest hot water temperature difference, effectiveness, and rate of heat transfer are observed for $\Theta = 30^\circ$ HCCHE, while the lowest values are attributed to $\Theta = 90^\circ$ HE. Tube side Nusselt numbers, pressure drops, and friction factors show agreement with the predictions of researchers. The analysis reveals that the coil fluid pressure drop is maximal for $\Theta = 0^\circ$ HE, whereas the maximum shell fluid pressure drop is encountered for $\Theta = 90^\circ$ HE. Furthermore, the highest pumping power per unit heat transfer area for coil and shell fluids are noted for $\Theta = 0^\circ$ HE and $\Theta = 90^\circ$ HE, respectively, while $\Theta = 30^\circ$ HCCHE exhibits comparable performance to the remaining HEs within the specified parameter range, establishing its optimality.

© 2024 The Author(s). Journal of Heat and Mass Transfer Research published by Semnan University Press.

This is an open access article under the CC-BY-NC 4.0 license. (<https://creativecommons.org/licenses/by-nc/4.0/>)

1. Introduction

Helical coil heat exchangers (HCHE) are used in chemical reactors, fire tube boilers, solar water heating systems, storage tanks, food and dairy industries, and heat recovery systems. In curved tubes, fluid at the center gets bifurcated into two streams, causing secondary flow vortices to occur. Dean No ($De = Re (CR^{0.5})$) takes into

account the existence of secondary flow [1]. The heat transfer rate and pressure drop are mainly dependent upon Reynolds number, Prandtl number, curvature ratio (CR), and Dean Number. Researchers investigated the heat transfer coefficient of the straight, helical coil (SHC) and spiral coils, and they found that they were higher than straight tubes [2, 3]. Naphon [4] also conducted investigations to compare SHC with

* Corresponding author.

E-mail address: magarsusheel@gmail.com

Cite this article as:

Magar, S. M., Gugliani, G. K. and Navthar, R. R., 2024. Experimental Heat Transfer Analysis of Helical Coiled Tubes on the Basis of Variation in Curvature Ratio and Geometry, 11(1), pp. 89-108.

<https://doi.org/10.22075/JHMTR.2024.32179.1491>

and without fins. Several Researchers [5-8] have studied natural convection and mixed convection in vertical straight helical coil heat exchangers (SHCHE). Ali [5] varied the number of turns (N) and pitch (P), keeping tube diameter (d_o) and coil diameter (D) fixed, and a constant temperature bath at the shell side was maintained. Ghorbani et al. [6,7] studied mixed convection of SHCHE by varying d_o , D, P, and N and keeping height and shell dimensions constant. Correlation to calculate modified effectiveness was proposed. Shokouhmand et al. [8] carried out experiments with three SHCs with variations in pitch and curvature ratio. They found that the shell-side heat transfer coefficients of the coils with larger pitches are more than the ones with smaller pitches.

In addition to examining various boundary conditions and working fluids other than water, several researchers [9-12] also looked at temperature-dependent fluid properties. Jaykumar JS et al. [9] concluded that for conjugate fluid-to-fluid heat transfer, better results were obtained than constant temperature and constant flux boundary conditions. Salimpour M [10] experimentally studied SHC, in which temperature-dependent properties of oil were considered. Kharat et al. [11] studied heat transfer characteristics of flue gas over the concentric helical coils. They demonstrated the importance of the Coil Gap ratio in heat transfer analysis. Moawad [12] studied experimentally the wall's constant heat flux boundary conditions made by electric heating. Forced convection is achieved by forcing air to flow over the outside surface of helically coiled tubes.

Helical cone coils are the subject of current research using experimental and numerical methods. Ke et al. [13] numerically investigated HCC and varied cone angle (θ) in the range of 55° to 85° while the cone base diameter was kept constant. They found that the coefficient of heat transfer of the circular cross-section was better than the elliptical. It was predicted that, from the base of the cone to the apex of the cone, for an increase in curvature ratio, the main flow or axial flow was increased, and for 0.1 m/s set value of flow speed, maximum velocity was observed as 0.1642 m/s. AboElazm et al. [14] compared HCC with SHC, considering two coils having heights of 0.04 m and 0.05 m, respectively. Exit temperature for HCC is found to be greater by 2.5-3.5°C than SHC. Daniel et al. [15] carried out experiments and numerical studies of single horizontal HCC. For $d_i=0.007904$ m, the base and top diameters were 0.150 m and 0.075 m, respectively. For these dimensions, Re_i is selected in the range of 4300 to 18600 to have flow in laminar and turbulent regimes. Vester et al. [16] presented a detailed review of

turbulent flow in coiled tubes. Basics of secondary flow, turbulent flow, and transition to turbulence were discussed. Jamshidi et al. [17] studied a conical geothermal heat exchanger in which heat exchangers were buried in soil at a depth of 3 m. They concluded that, for conical coil, Nu and outlet temperature were found to be increased for an increase in coil diameter, cone angle, and Reynolds number. Daghigh et al. [18] experimentally investigated three coils, including SHC, HCC, and conical-cylindrical- spiral, and used working fluids as nanofluids- MWCNT, CuO, TiO₂, and water. The conical-cylindrical-spiral coil was observed to perform better than other coils. Palanisamy et al. [19] experimentally investigated the heat transfer coefficient and pressure drop of horizontal HCC. Multi-wall carbon nanotubes/ water nanofluids were used. It was predicted that for water having dean no. in the range of 2225- 4300, pressure drop was found to be in the range of 8000-13000 Pa. Heyhat MM et al. [20] experimentally studied HCC for variation of cone angle in the range of 30° , 45° , 60° and 90° . SiO₂/water nanofluid was allowed to pass through the tube, and the outer surface of the coil was heated. It was predicted that coil pitch variation was less effective for heat transfer enhancement than cone angle variation. Ali et al. [21] numerically simulated double pipe HCCHE to obtain the annulus side friction factor and Nusselt number. It was concluded that for an increase in cone angle from 0° to 90° , Nu_i and friction factor increased by 31.71% and 15.51%. Sheeba et al. [22] experimentally and numerically investigated double-pipe HCCHE. Experimentation was carried out for HCC, which had a cone angle of 72° , and numerically, the cone angle varied from 30° to 90° . It was predicted that, as the cone angle was increased, the overall heat transfer coefficient would increase up to 72° cone angle. With a further increase in the cone angle, the overall heat transfer coefficient was found to decrease. AlSalem et al. [23] numerically studied tube-in-tube conical heat exchangers, keeping the conical coil in an inverted position, i.e., the apex of the cone facing towards the ground. It was concluded that maximized exergy efficiency was found for minimum values of cone angle (range- 0° , 45° , 90° , 135°). Maghrabie et al. [24] studied a single SHC in which the inclination angle was varied in the steps of 10° from the horizontal direction (0°) to the vertical direction (90°). Dean number was varied in the range of 1540 to 3860. It was predicted that for vertical position, effectiveness was 23.1 % and 11 % more than horizontal position for Dean number 1540 and 3860, respectively. Chokphoemphun et al. [25] studied coil tube exchangers kept inside the freeboard zone of a fluidized bed combustor. The outside

surface of the coil was heated by flue gasses flowing from the bottom, and the air was allowed to flow through the coil. It was depicted that the outlet temperature of air for parallel flow was found to be greater than counter flow by 7-17°C. Hassan and Mostafa [26] experimentally studied forced convection in SHCHE. Keeping the surface area of the coil fixed, tube diameter, coil diameter, and pitch were varied. For five tube diameters and six coil diameters, four variations in pitch were studied. It was predicted that Nu_i enhanced with higher values of D/d_o . Also, an optimum value of D/d_o was observed, after which Nu_i was found to decrease with the increase in D/d_o . Also, a correlation to calculate Nu_i was proposed. A study of the effect of nanofluids over thermal and hydrodynamic parameters in other types of heat exchangers is also going on. Hassaan [27] experimentally studied plate-type heat exchangers using multi-wall carbon nanotubes (MWCNT) and distilled water with 05 volume concentrations (0.22 % to 1.5 %). Reynolds number range of heated nanofluids and distilled water was considered as 100 to 700. It was predicted that the increase in Nu would reach 32 % for nanofluids with a volume concentration of 1.53%. In addition to this, Hassaan A [28] carried out a study of the effect of hybrid nanofluids (MWCNT- Al_2O_3 /water) in plate-type heat exchangers. Effectiveness, U , Nu , ΔP , and friction factor were computed. Sharma et al. [29] experimentally and numerically studied a helical coil cavity receiver (used in process heating applications) having a conical shape. Coating was done by using nanostructured carbon florets. Maximum efficiency was achieved at a cone angle of 40° when the radial pitch to tube diameter was equal to 1. Also, Hassaan [30] experimentally examined shell and tube-type heat exchangers (STHE). Heated MWCNT and distilled water were allowed to flow through the tubes. It was predicted that Nu_i for nanofluids was 55.6% higher than that of distilled water. In the case of distilled water for the Re_i range of 2500 to 12500, Nu_i was obtained in the range of 10 to 25, for said range of Re_i pressure drop and f_i were obtained in the range of 125-230 Pa and 0.009- 0.002 respectively. Hassaan [31, 32] compared STHE with a tubular heat exchanger (TTE). MWCNT nanofluid / distilled water with three-volume concentrations was used. The comparison was made on the basis of the same heat transfer area and the same mass flow rates. It was proposed that the heat transfer of STHE was 7- 43 % higher than CTE. Comparisons of Nusselt number showed that CTE had higher Nu in the range of 28.5-40%.

Omri et al. [33] experimentally studied single SHC using distilled water-based CuO-Gp (80-20%) hybrid nanofluid in a laminar flow regime

($768 \leq Re \leq 1843$). It was predicted that an increase in Re_i improved h_i , and this improvement was more at the coil entrance region. Alklaibi A. et al. [34] experimentally investigated horizontal SHC in which hot water was allowed to flow in the shell, and ethylene glycol mixture-based Fe_3O_4 was made to flow in the coil as a coolant. It was predicted that at 2.0 % nanoparticle concentration, the maximum increase of U was found to be 4.27 % than that of the base fluid. Mustafa et al. [35] presented a review of the effect of the use of nanofluids on the thermal characteristics of helical coils. The review consisted of a discussion of experimental and numerical studies carried out using various nanofluids for vertical straight, helical coils, and conical coils.

A comparative analysis of helical coiled tube heat exchangers on the basis of gain in thermal performance against pressure drop, pumping power, and pumping power per unit heat transfer area was not found. In the case of the vertical helical coil (HCC), enough work is not found when the coil is kept in such a way that its apex is facing the ground. Actually, in this position, when fluid flows from a bigger coil diameter (base side diameter) towards a smaller coil diameter (apex side diameter), its flow is taken in the direction of increasing curvature. This is not discussed earlier. For coiled heat exchangers, not enough work has been reported on the study of the effect of variation of CR and geometry on thermal performance, hydrodynamic performance, and prediction of optimum heat exchangers.

To investigate this, it is intended to study coiled heat exchangers experimentally. The thermal and hydrodynamic analysis is done by selecting HCC, spiral, and SHC in which cone angle (θ) is varied between 90° to 0° in the steps as 70°, 50°, and 30° for all types of heat exchanger's coil side volume are kept same. Similarly, the shell side volume is also fixed. For SHC, coil diameter (D) is considered to be 0.07 m ($CR=0.14$). The same value of D is considered for the smaller end diameter of HCC and spiral coil. Then, for fixed length and variation in θ , bigger end diameters are obtained. As a result of this, a wide range of CR is obtained as 0.028 to 0.14. The optimized heat exchanger is predicted on the basis of thermal and hydrodynamic parameters. Thermal parameters selected as outlet temperature of hot water ΔT_{ch} , effectiveness, rate of heat transfer Q_{ch} Nusselt number. Similarly, hydrodynamic parameters are considered as pressure drop of the coil and shell fluid (ΔP_{ch} and ΔP_{sc}), tube side friction factor, Pumping power, and pumping power per unit heat transfer area. A schematic diagram of the HCCHE heat exchanger considered apex facing towards the ground is shown in Fig. 1. Also, variation of cone angle (θ) is shown schematically in Fig. 2.

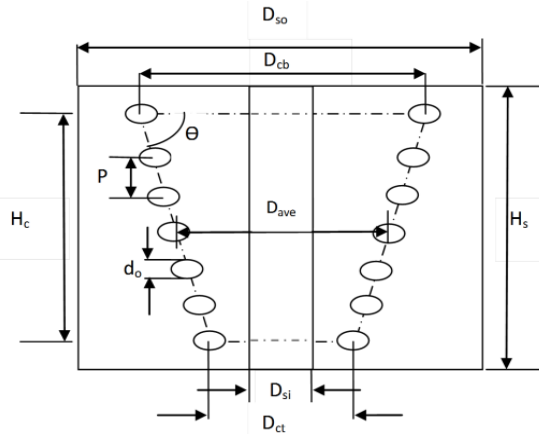


Fig. 1. Schematic diagram of helical cone coil heat exchanger (HCCHE)

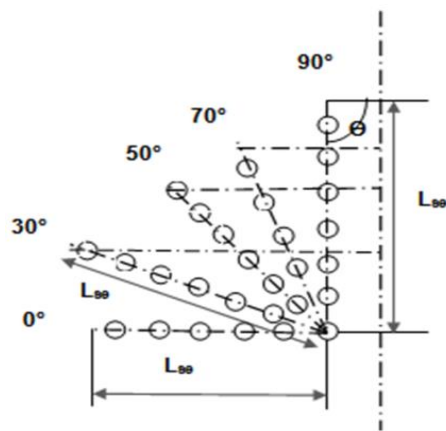


Fig. 2. Variation of cone angle, θ

2. Experimentation

The experimental setup was created using multiple parts illustrated in Fig. 3. Fig. 4 displays

a photograph of the manufactured setup. From hot and cold-water tanks, respectively, hot and cold water was forced into the coil and shell. Tanks were equipped with float and solenoid valves to maintain a constant water level within. The hot water tank and heat exchangers were insulated. The water in the hot water tank was heated utilizing an electric heater, and a thermostat kept the temperature constant. RTD thermocouples were used to measure the temperatures at the inlet and exit. The accuracy of RTD thermocouples is $100 \pm 0.5^\circ\text{C}$. Temperature of hot water inside the tank is displayed at location I1. Similarly, hot and cold water's inlet and exit temperatures are indicated at locations I2, as shown in Fig. 3. Readings from the data logger were recorded and sent to the computer. U-tube manometers were used to measure the pressure drop of the coil and shell fluids [19]. The shell was made of mild steel. Copper tubes were used to make cone coils. Wooden cones were produced for each coil. The sand was filled into every copper tube that was wound around a respective wooden cone. The minimum coil diameter was selected as 0.07 m to preserve the tube's circular cross-sections in all coils. In SHCHE ($\theta=90^\circ$), D_{ave} was considered to be 0.07 m. This has given the maximum CR of 0.14. For a variation of θ from 70° to 0° , a smaller end diameter, D_{ct} , was maintained constant at 0.07 m, and an equivalent bigger end diameter, D_{cb} , was obtained for a fixed length of the coil. Keeping inner shell diameter, $D_{si}=0.02$ m constant, outer shell diameter, D_{so} , and height of shell, H_s were obtained for every heat exchanger, keeping shell side volume fixed. Dimensions of heat exchangers are presented in Table 1.

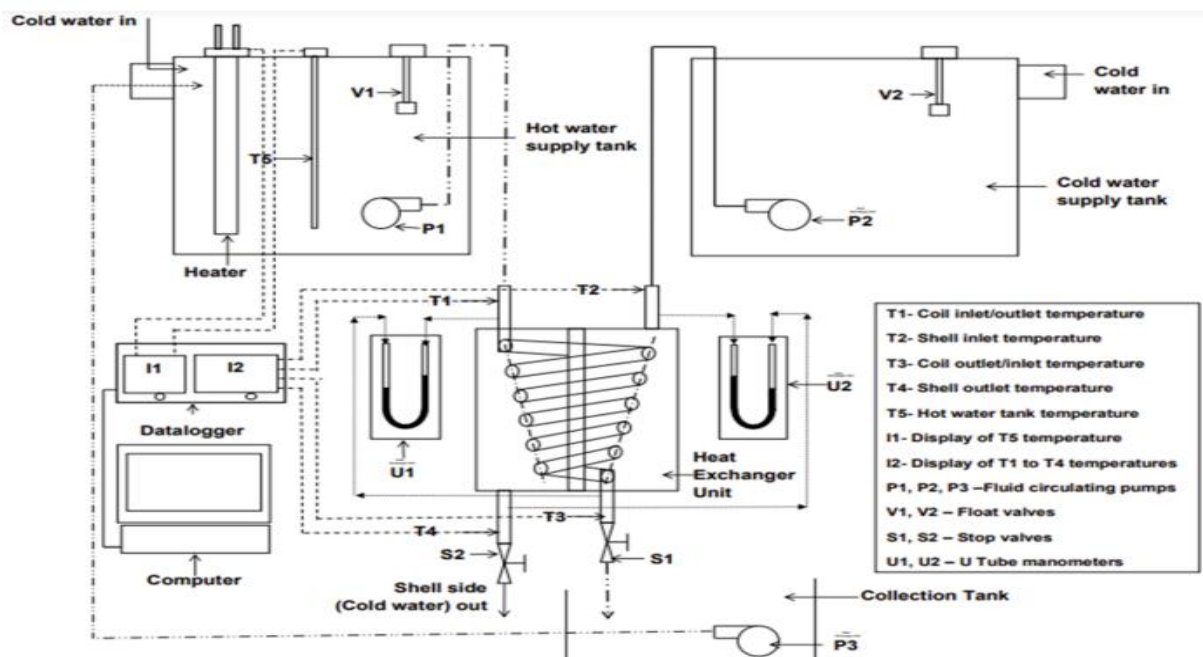


Fig. 3. Schematic diagram of Heat exchanger test rig



Fig. 4. Photograph of Heat exchanger test rig

Table 1. Dimensions of heat exchangers

Parameter	Dimension				
Tube inner diameter, d_i , m	0.01				
Top diameter, D_{ct} , m	0.07				
Pitch, P , m	0.018				
Tube length, L_c , m	3.3				
Inner shell diameter, D_{si} , m	0.02				
Cone angle, θ	90°	70°	50°	0°	30°
Base diameter, D_{cb}	0.07	0.17	0.25	0.27	0.35
Average diameter, D_{ave}	0.07	0.12	0.16	0.17	0.21
Curvature ratio, CR_{base}	0.14	0.059	0.040	0.037	0.028
Curvature ratio, CR_{ave}	0.14	0.083	0.063	0.059	0.048
Outer shell diameter, D_{so} , m	0.24	0.3	0.33	0.42	0.38
Slant edge length, L_{se} , m	0.24	0.18	0.21	0.20	0.29

SHC coil diameter was present close to D_{si} . For the heat exchangers having $\theta = 70^\circ, 50^\circ, 30^\circ$, and 0° , D_{ct} and D_{cb} were near to D_{si} and D_{so} , respectively. Furthermore, the D_{ave} of these conical heat exchangers was present near the center of the shell. As a result of this, for these helical cone coils, the maximum portion of shell fluid remained in contact with the coil compared to SHCHE ($\theta=90^\circ$).

Mass flow rates of the coil fluid were chosen in a way that assured laminar or turbulent flow through the tube. Re_{crit} , which was calculated using Eq. no. 11, determined whether a flow was laminar or turbulent. Re_i for laminar flow is between 3700 and 3900. Similarly, the Re_i range for turbulent flow is 13000–20000. Table 2 provides information on the flow parameters used in the tests.

Table 2. Flow parameters of heat exchangers

Parameter	Range
Mass flow rates (Coil- Hot water), m_{ch} , kg/s	0.02 – 0.1
Mass flow rates (Shell- Cold water), m_{sc} , kg/s	0.02- 0.1
Inlet temperature (Coil- Hot water), T_{ch} , °C	42 ±0.5
Inlet temperature(Shell- Cold water), T_{sc} , °C	27.5 ±0.5
Tube side Reynolds number, Re_i	3700-20000
Tube side Dean number, De_i	800-7500

The inflow of cold water into the shell was fixed from the top in all testing runs. Hot water was forced to enter the tube from the top in parallel flow, while in counter flow, the fluid entered the tube from the bottom. To measure the mass flow rate, a measuring cylinder and stopwatch were positioned at the exit of the heat exchanger. [6,7] With the use of a data collection system, the inlet and outlet temperatures of coil and shell fluids were monitored every minute. Readings were recorded after the steady state condition was reached. Uncertainties were used to provide accuracy of the experimental results, and the method proposed by Kline and McClintock [36] was adopted for the calculation of uncertainties, which is widely accepted by researchers. Uncertainty values of various variables are presented in Table 3. These values lie within acceptable limits.

Table 3. Uncertainty values

Parameter	Uncertainty (%)
Mass flow rates	4.1
Reynolds number	4.5
Dean number	4.5
Friction factor	4.6
Rate of heat transfer	4.3
Nusselt number	4.3

3. Data Reduction

Hot water and cold water were forced to flow through coil and shell respectively, heat transfer takes place from hot water to cold water through tube walls.

Heat rejected by hot water is obtained as

$$Q_{ch} = (mCp)_{ch} \cdot (T_{hi} - T_{ho}) \quad (1)$$

where T_{hi} and T_{ho} were temperatures of hot water recorded at the entrance and exit of the coil.

Similarly, heat absorbed by cold water is calculated as

$$Q_{sc} = (mCp)_{sc} \cdot (T_{co} - T_{ci}) \quad (2)$$

where T_{ci} and T_{co} were temperatures of cold water recorded at entrance and exit of the shell.

According to energy balance, heat rejected by hot water is equal to heat absorbed by cold water.

$$Q_{ch} = (mCp)_{ch} \cdot (T_{hi} - T_{ho}) = Q_{sc} = (mCp)_{sc} (T_{co} - T_{ci})$$

Readings were recorded when steady state was achieved and energy balance was observed for $Q_{ch}/Q_{sc}=1 \pm 0.5$.

Average rate of heat transfer (Q_{ave}) is calculated as average of Q_{ch} and Q_{cs} [30].

Overall heat transfer coefficient U is calculated on the basis of LMTD

$$U_{i/o} = \frac{Q_{ch}}{A_{i/o} LMTD}$$

LMTD is given as,

$$LMTD = \frac{\Delta T_1 - \Delta T_2}{\ln \frac{\Delta T_1}{\Delta T_2}}$$

For parallel flow,

$$\Delta T_1 = T_{hi} - T_{ci} \text{ and } \Delta T_2 = T_{ho} - T_{co}$$

For counter flow,

$$\Delta T_1 = T_{hi} - T_{co} \text{ and } \Delta T_2 = T_{ho} - T_{ci}$$

Performance of heat exchanger is measured by effectiveness, ϵ as [6]:

$$\epsilon = \frac{Q_{actual}}{Q_{max}} \quad (3)$$

where Q_{actual} is actual heat transfer rate and given as

$$Q_{actual} = Q_{ch} = (mCp)_{ch} (T_{hi} - T_{ho}) = Q_{sc} = (mCp)_{sc} (T_{co} - T_{ci}) \quad (4)$$

and Q_{max} is maximum heat transfer rate and given as

$$Q_{max} = (mCp)_{min} (T_{hi} - T_{ci}) \quad (5)$$

Effectiveness is then written as,

$$\epsilon = \frac{Q_{ch} = Q_{sc}}{Q_{max}} = \frac{(mCp)_{ch} (T_{hi} - T_{ho}) = (mCp)_{sc} (T_{co} - T_{ci})}{(mCp)_{min} (T_{hi} - T_{ci})} \quad (6)$$

$$\text{If } (mCp)_{min} = (mCp)_{ch}; \epsilon = \frac{T_{hi} - T_{ho}}{T_{hi} - T_{ci}} \quad (7)$$

$$\& (mCp)_{min} = (mCp)_{sc}; \epsilon = \frac{T_{co} - T_{ci}}{T_{hi} - T_{ci}} \quad (8)$$

Few researchers studied modified effectiveness (ϵ') for coiled heat exchanger which is calculated as [6,38]:

$$\epsilon' = \frac{T_{hi} - T_{co}}{T_{hi} - T_{ci}} \quad (9)$$

Tube side Curvature Ratio considering average diameter of cone coil (D_{ave}) are obtained as:

$$CR = \frac{d_i}{D_{ave}} \quad (10)$$

where D_{ave} is the average diameter obtained from D_{cb} and D_{ct} as

$$D_{ave} = \frac{D_{cb} + D_{ct}}{2}$$

For SHC i.e. $\theta=90^\circ$, $D_{ave} = D_{cb} = D_{ct}$ (In this study $D_{ct}=0.07m$). Also for spiral coil ($\theta = 0^\circ$), D_{ave} is

obtained as average of inner and outer diameter of horizontal spiral coil.

Re_i and corresponding De_i are calculated using the following formulation.

$$Re_i = \frac{\rho_{ch} \cdot v_{ch} \cdot d_i}{\mu_{ch}}$$

$$De_i = Re_i \cdot CR_{ave}^{0.5}$$

On the basis of Re_{crit} type of flow inside tube is decided as laminar or turbulent. Following Schmidt's formula for Re_{crit} is preferred [37].

$$Re_{crit} = 2300 \cdot (1 + 8.6 \cdot (CR^{0.45})) \quad (11)$$

For the laminar and turbulent flow, the Wilson plot technique is used to obtain heat transfer coefficients and Nusselt numbers. While applying the Wilson plot method, it was decided to keep the mass flow rate of hot water in the tube fixed, and the mass flow rate of cold water in the shell was varied in four steps. It was assumed that for constant tube side mass flow rate, tube side heat transfer coefficient (h_i) remains constant. Shell side heat transfer coefficients (h_o) are proportional to the velocity of shell side fluid (v_s) such that h_o is equal to C.v_sⁿ. Then, the overall heat transfer coefficients U is plotted against v_sⁿ. The best linear fit is obtained by selecting proper values of exponent n. From the linear equation, values of h_o and h_i are obtained. Further tube side Nusselt number (Nu_i) and shell side Nusselt number (Nu_o) are obtained using the following formulae.

$$Nu_i = \frac{h_i \cdot d_i}{k_{ch}}; Nu_o = \frac{h_o \cdot D_{eq}}{k_{sc}} \quad (12)$$

In addition, friction factor for coil side fluid is obtained as [39]:

$$f = \frac{1}{2} \cdot \frac{\Delta P}{L} \cdot \frac{d_i}{\rho \cdot v_c^2} \quad (13)$$

where ΔP is the pressure drop. It is calculated using z as the height difference of mercury in the U tube manometer.

$$\Delta p = \rho \cdot g \cdot z \quad (14)$$

The fluid pumping power, PP is calculated as [39]:

$$PP = \frac{m\Delta P}{\rho\eta_p} \quad (15)$$

For the heat transfer area of every coil, pumping power per unit heat transfer area is calculated [39].

$$\frac{PP}{A} = \frac{m\Delta P}{A \cdot \rho\eta_p} \quad (16)$$

Validation is done in two ways. In the first way, values of the rate of h_i and h_o are obtained in such a way that by using these values of h_i and h_o, the heat transfer rate (Q_{wp}) is again calculated

using the same LMTD. A comparison of Q_{ave} is done with Q_{ch}. In the second way, Nu_i and tube side friction factor (f_i) obtained in this study are compared with the predictions of existing researchers for the selected range of parameters. For the comparisons of Nu_i for turbulent and laminar flow, the following correlations proposed by researchers are selected. Sigalotti et al. [40] discussed Mori and Nakayama's correlation for turbulent flow. It is given below, along with correlations from other researchers.

Mori and Nakayama's correlation for turbulent flow, Pr_i>1 and (Re_i.CR²)> 0.4 [40]

$$Nu_i = \frac{Pr_i^{0.4} \cdot Re_i^{5/6} \cdot (d_i/D)^{1/12} \cdot [1 + \frac{0.061}{(Re_i \cdot (d_i/D)^{2.5})^{0.167}}]}{41} \quad (17)$$

Pratt's correlation for turbulent flow [41]

$$Nu_i = 0.0225 \cdot \left[1 + 3.4 \cdot \left(\frac{d_i}{D}\right)\right] \cdot Re_i^{0.8} \cdot Pr_i^{0.4} \quad (18)$$

Schmidt's correlation for laminar flow, 100 < Re_i < Re_{crit} [42, 43]

$$Nu_i = 3.65 + 0.08 \cdot \left[1 + 0.8 \cdot \left(\frac{d_i}{D}\right)^{0.9}\right] \cdot Re_i^{0.5+0.2903\left(\frac{d_i}{D}\right)^{0.194}} \cdot Pr_i^{1/3} \quad (19)$$

Similarly for laminar and turbulent flow tube side friction factors (f_i) are compared with f_i obtained from correlations of Srinivasan, Mishra and Gupta.

Srinivasan's correlation for laminar flow, De_i> 300 and 7 < d_i/D < 104 [39]

$$f_i = \left(\frac{16}{Re_i}\right) \cdot 0.1125 \cdot De_i^{0.5} \quad (20)$$

Srinivasan's correlation for turbulent flow, [44]

$$f_i = 0.084 \cdot \left(\frac{d_i}{D}\right)^{0.1} \cdot Re_i^{-0.2} \quad (21)$$

Mishra and Gupta's correlation for turbulent flow, [37]

$$f_i = \frac{0.3164}{Re_i^{0.25}} \cdot [1 + 0.095 \cdot \left(\frac{d_i}{D}\right)^{1/2} \cdot Re_i^{1/4}] \quad (22)$$

4. Results and Discussion

4.1. Hot Water Temperature difference (ΔT_{ch}, °C):

In Fig. 5, the temperature difference of hot water (ΔT_{ch}) flowing through the coil is plotted against shell-side cold water mass flow rates

($m_{sc}=0.02$ to 0.1 kg/s). Figs. 5 (a) and 5(b) show ΔT_{ch} for laminar flow ($m_{ch}=0.02$ kg/s, $Re_i= 3700$) for parallel and counter flow configurations, respectively. It is observed that, as cold water mass flow rate is increased, the exit temperature of hot water ($T_{ch,o}$) is found to decrease. Due to this, the hot water temperature difference is increased for increments in cold water mass flow rate.

Also, the highest ΔT_{ch} is found for laminar flow ($m_{ch}=0.02$ kg/s) in parallel flow arrangement. The reason behind this is that as the cold water mass flow rate is increased, the rate of heat transfer, Q_{sc} ($Q_{sc}=Q_{ch}$), is found to be increased. At lower values of m_{ch} (0.02 kg/s), to compensate for this rise in heat rate, ΔT_{ch} is found to be increased. Similarly, when hot water is flowing in a turbulent regime ($m_{ch}=0.1$ kg/s, $Re_i= 20000$), values of heat capacities are at higher levels, causing smaller values of ΔT_{ch} . Hence, for hot water flow in a turbulent regime, ΔT_{ch} is found to be lower than laminar flow (As shown in Figs. 5 (c) and 5(d)).

Also, it is observed that for parallel flow arrangement and when hot water is flowing in a laminar regime, for $\theta =30^\circ$ HCCHE, ΔT_{ch} is higher by 18 % than $\theta =90^\circ$ SHCHE and by 7% than $\theta =0^\circ$ HE. In addition, when hot water is flowing in a turbulent regime, for $\theta =30^\circ$ HCCHE, ΔT_{ch} is higher by 34 % than $\theta =90^\circ$ SHCHE and by 24% than $\theta =0^\circ$ HE. For $\theta =70^\circ$ and 50° HCCHEs, ΔT_{ch} is found in between $\theta =90^\circ$ SHCHE and $\theta =0^\circ$ HE. Thus, the highest ΔT_{ch} is found for $\theta =30^\circ$ HCCHE, and the lowest ΔT_{ch} is found for $\theta =90^\circ$ SHCHE. This is because for $\theta =90^\circ$ SHC, the coil diameter is equal to 0.07 m, and it is positioned very close to the inner shell of the heat exchanger (the diameter of the inner shell is 0.02 m). But for $\theta =30^\circ$ HCC, the average diameter is 0.21 m, which is positioned at the center of space between the inner shell and the outer shell. Thus, for parallel flow configuration, due to conical geometry with the longest slant edge, effective contact of shell fluid takes place with the tube surface. Due to this, the exit temperature of hot water is decreased by increments in shell cold water mass flow rate.

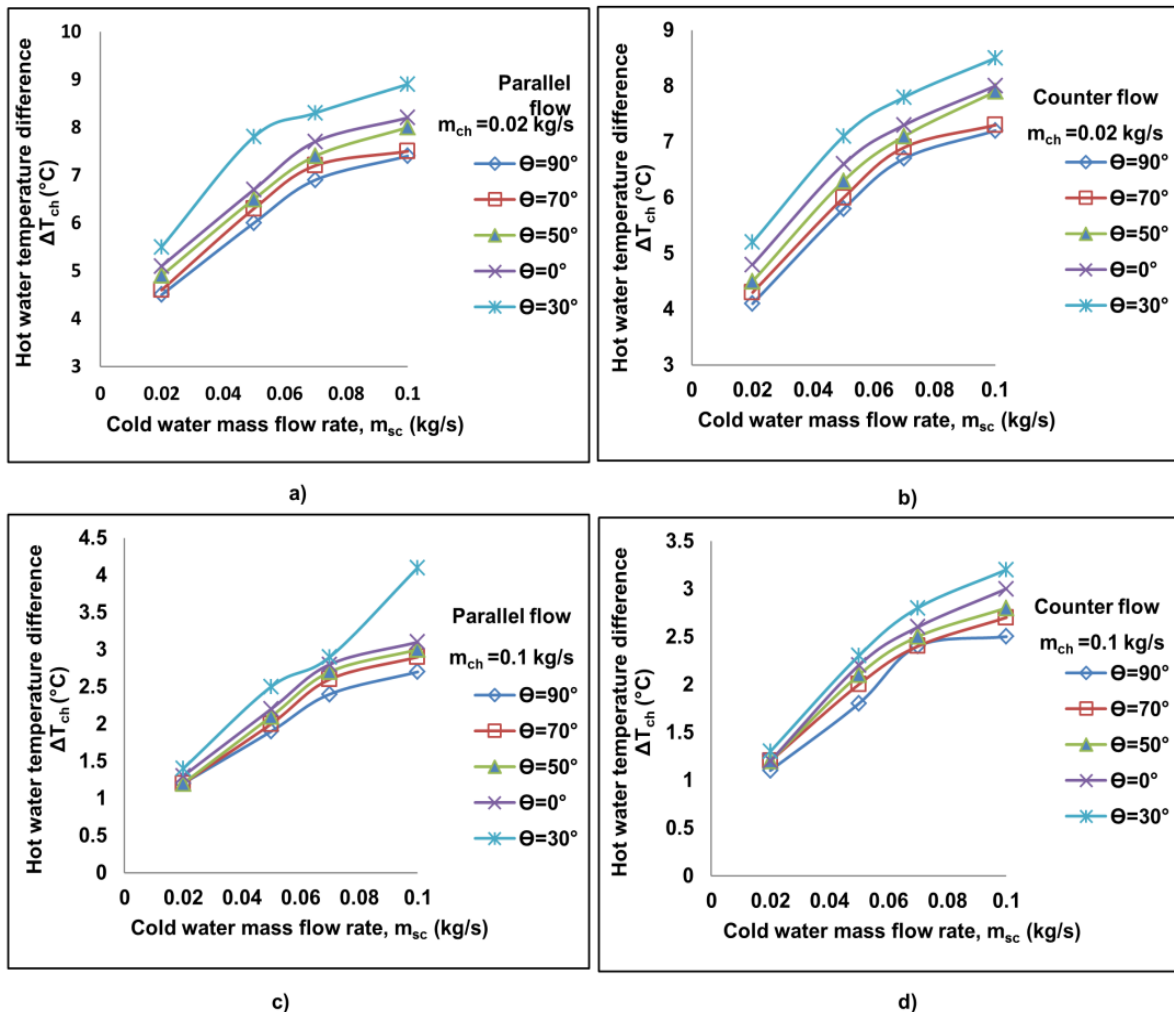


Fig. 5. Hot water temperature difference with respect to cold water mass flow rate

4.2. Effectiveness

Effectiveness is calculated by using Eq. no. 3. In Fig. 6, the effectiveness is plotted against shell side cold water mass flow rate when tube side hot water flows are in laminar and turbulent regimes. Fig. 6 (a) and (b) indicate variations in effectiveness for parallel and counter flow when hot water flows in a laminar regime ($m_{ch} = 0.02$ kg/s). For laminar flow, effectiveness is found to increase when the mass flow rate of cold water is increased from 0.02 to 0.1 kg/s. The highest effectiveness is obtained for laminar flow in parallel flow configuration. The reason behind this is explained as: a) for laminar flow, the highest ΔT_{ch} is obtained. b) For laminar flow, the lowest heat capacities are present for hot water. Hence, in the formulation of effectiveness, the highest ΔT_{ch} is considered in the numerator, causing the highest effectiveness.

In the case of turbulent flow ($m_{ch} = 0.1$ kg/s), effectiveness is found to be decreased when the cold-water mass flow rate is increased from 0.02 to 0.1 kg/s. It is shown in Fig. 6 (c) and (d). Heat

capacity is highest for the turbulent flow of hot water, and when the mass flow rate of cold water increases from 0.02 to 0.1 kg/s, the heat capacities of cold water also increase from minimum to maximum values. Due to this, the temperature difference of cold water (ΔT_{sc}) must be taken into consideration while calculating effectiveness. But ΔT_{sc} is found to be decreased as the cold-water mass flow rate is increased. Thus, due to a lower value of ΔT_{sc} , a decrease in effectiveness is found.

For $\theta = 30^\circ$ HCCHE, the highest effectiveness is obtained as 0.61 in parallel flow arrangement having laminar flow. Also, for $\theta = 30^\circ$ HCCHE and hot water flowing in a laminar regime, effectiveness is 14% higher than $\theta = 90^\circ$ SHCHE and by 7% than $\theta = 0^\circ$ HE, respectively. Similarly, for turbulent flow the highest effectiveness is obtained as 0.49 for $\theta = 30^\circ$ HCCHE. Also, for $\theta = 30^\circ$ HCCHE and hot water flowing in a turbulent regime, effectiveness is 15% higher than $\theta = 90^\circ$ SHCHE and by 7% than $\theta = 0^\circ$ HE, respectively.

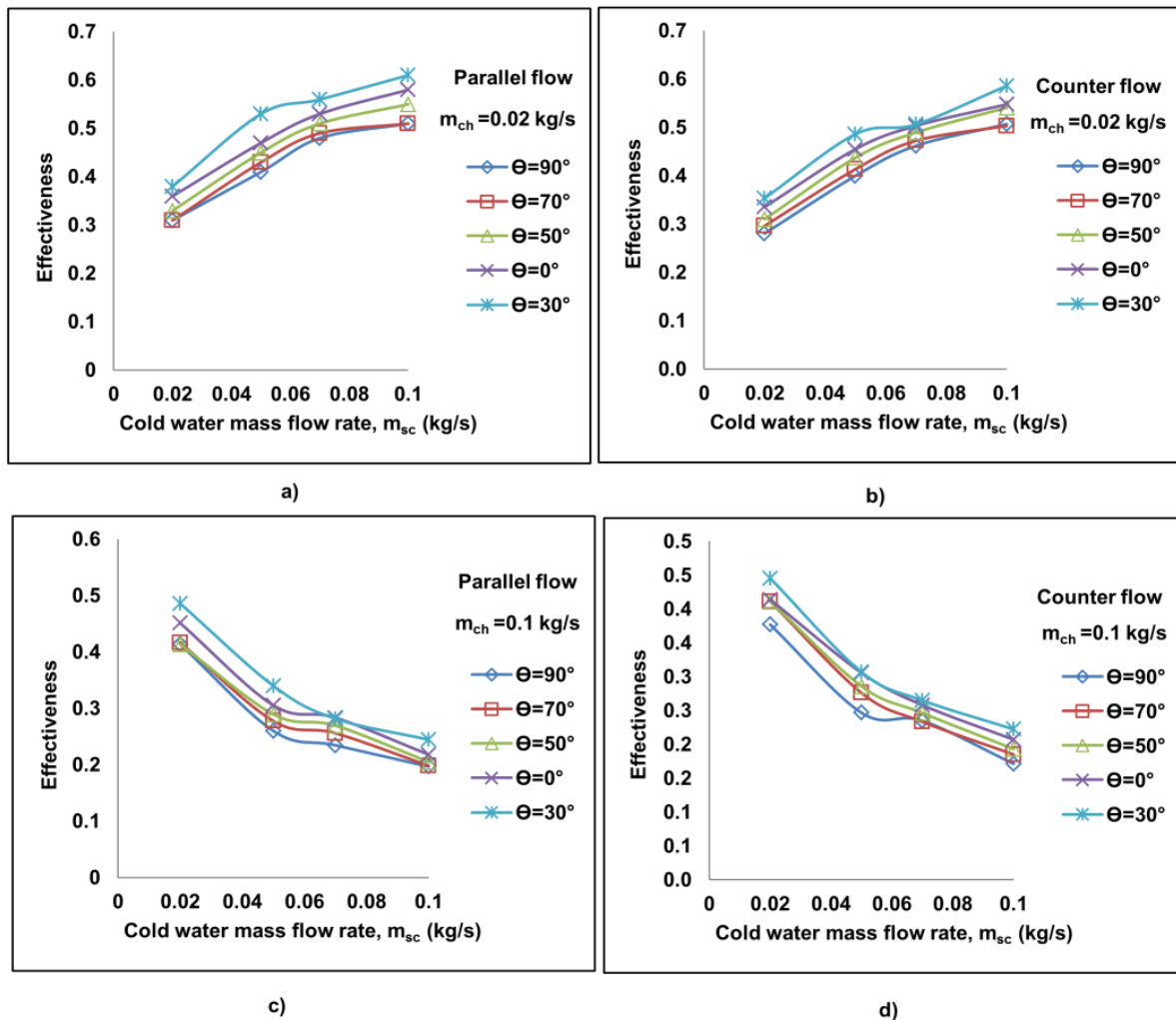


Fig. 6. Effectiveness with respect to cold water mass flow rate

In addition to this, modified effectiveness (ϵ') is also studied here. Modified effectiveness gives comparison of cold water exit temperature ($T_{sc,o}$) for similar inlet conditions. Modified effectiveness is obtained as per Eq. no. 9. It is plotted versus ratio of mass flow rates (m_{ch}/m_{sc}) and shown in Fig. 7. Graphs show that ratio of mass flow rates (m_{ch}/m_{sc}) increases ϵ' is found to be decreased. The agreement is found with the results of Ghorbani et al. [6] and Purandare et al. [38]. Purandare et al. [38] obtained the highest ϵ' for SHC and lowest ϵ' was obtained for the spiral coil. Similar to these results the highest ϵ' is obtained for $\theta = 90^\circ$ SHCHE and lowest ϵ' is obtained for $\theta = 0^\circ$ HE (spiral coil). Ghorbani et al. [6] studied mixed convection in SHC and proposed a correlation to obtain ϵ' . While proposing the correlation range of ratio of mass flow rates (m_{ch}/m_{sc}) was considered as: $0.3 < m_{ch}/m_{sc} < 5$.

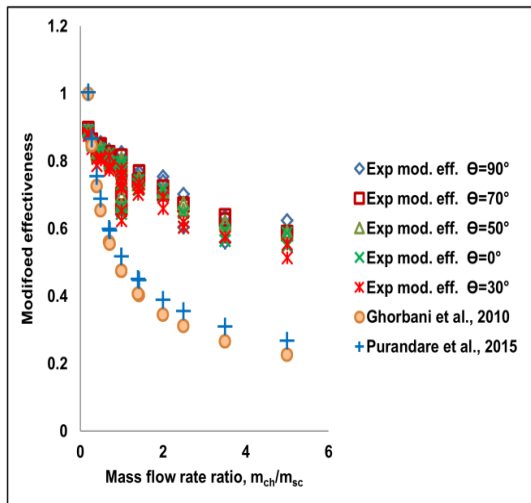


Fig. 7. Modified effectiveness with respect to ratio of mass flow rates.

Also Purandare et al. [38] proposed correlations to obtain ϵ' . A lower range of m_{ch}/m_{sc} was considered. These correlations for SHC are given below.

Correlation of Ghorbani et al. [6],

$$\epsilon' = 0.4744 * \left(\frac{m_{sc}}{m_{ch}}\right)^{0.4627} \tag{23}$$

Correlation of Purandare et al. [38],

$$\epsilon' = 0.5177 * \left(\frac{m_{sc}}{m_{ch}}\right)^{0.4114} \tag{24}$$

By using these correlations ϵ' is obtained for parameters studied here and compared with experimental results of this study. This is shown in Fig. 7. It is found that ϵ' obtained experimentally for this study is on the higher side than that are obtained from the above

correlations. Higher values of ϵ' means higher exit temperature of shell side cold water ($T_{sc,o}$). Thus in this study forced convection is studied for a higher range of m_{ch}/m_{sc} as $0.2 \leq m_{ch}/m_{sc} \leq 5$. Correlation for ϵ' is proposed for all heat exchangers using a simple power equation. This equation is given below.

$$\epsilon' = a * \left(\frac{m_{sc}}{m_{ch}}\right)^b \tag{25}$$

values of constant a and b are mentioned in Table 4. Experimental values of ϵ' are compared with values obtained from the correlation. Maximum variation is found to be 15 %. Hence ϵ' may be used in the design process of the coiled tube heat exchanger.

Table 4. Constants for modified effectiveness, ϵ' correlation

Constants	$\theta = 90^\circ$	$\theta = 70^\circ$	$\theta = 50^\circ$	$\theta = 0^\circ$	$\theta = 30^\circ$
a	0.7625	0.7574	0.7507	0.7385	0.7199
b	0.1289	0.1260	0.1271	0.1425	0.1503
R ²	0.80	0.86	0.88	0.83	0.85

4.3. Rate of Heat Transfer, Q_{ch}

Q_{ch} is the rate of heat rejected by coil side hot water to shell side cold water. Fig. 8 shows graphs of Q_{ch} versus cold water mass flow rate. As expected, Q_{ch} increases as m_{sc} increases. The highest Q_{ch} is obtained at $m_{sc}=0.1$ kg/s for turbulent hot water flow. Also, variations in Q_{ch} are occurred predominantly at $m_{sc}=0.1$ kg/s for all heat exchangers. Q_{ch} is higher for parallel flow than counter flow. For $\theta = 30^\circ$ HCCHE and hot water flowing in a laminar regime, Q_{ch} is 17 % higher than $\theta = 90^\circ$ SHCHE and by 8 % than $\theta = 0^\circ$ HE, respectively. Similarly, for turbulent flow, Q_{ch} for $\theta = 30^\circ$ HCCHE is 23 % higher than $\theta = 90^\circ$ SHCHE and by 11 % than $\theta = 0^\circ$ HE, respectively. For $\theta = 70^\circ$ and 50° HCCHEs, Q_{ch} lies between $\theta = 90^\circ$ SHCHE and $\theta = 0^\circ$ HE.

Further in this study the Wilson plot method is used to obtain values of tube side and shell side heat transfer coefficients (h_i and h_o). These values of h_i and h_o are used to obtain the overall heat transfer coefficient, U, and using the same LMTD, again the rate of heat transfer is calculated. This rate of heat transfer is labelled as Q_{wp} . Then $((Q_{ave} - Q_{wp} / Q_{ave}).100)$ is obtained to check the relevance of values of h_i and h_o obtained from Wilson plots. It is found that for selected values of h_i and h_o , $((Q_{ave} - Q_{wp} / Q_{ave}).100)$ is found to be within 7%. These values of h_i and h_o are further used to obtain tube side and shell side Nusselt numbers (Nu_i and Nu_o).

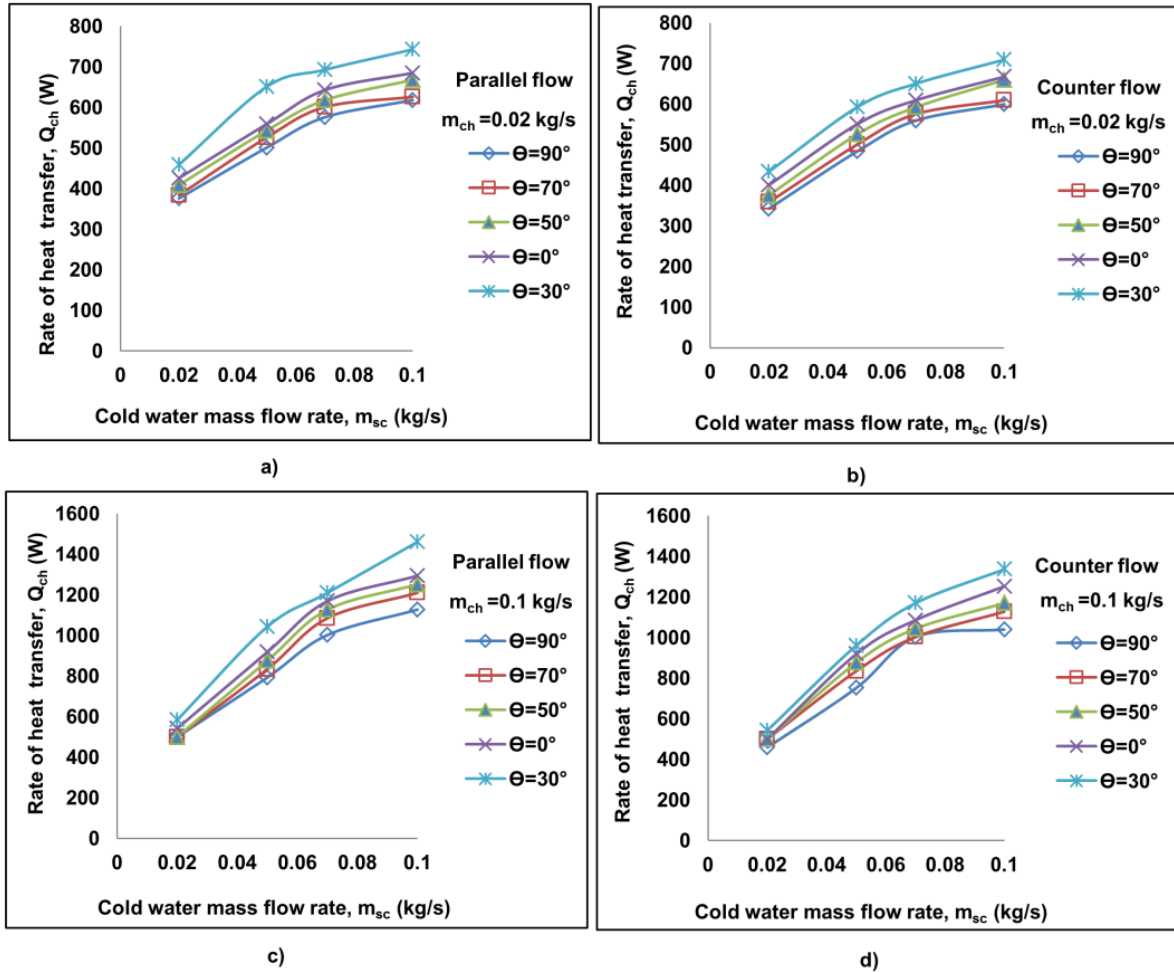


Fig. 8. Rate of heat transfer with respect to cold water mass flow rate

Nu_i is plotted against Re_i for variation of CR. It is shown in Fig. 9. As expected, Re_i increases, and Nu_i is found to increase. This is in agreement with Haassaan [26]. Secondary flows are generated due to the centrifugal action of fluid flowing in curved tubes. Due to an increase in tube side velocities and curvature ratio, secondary flows become intensive. This reduces the laminar boundary layer, which enhances convection. It is observed that as CR increases, Nu_i is found to increase. Maximum Nu_i is obtained for average CR = 0.14. This indicates that the effect of secondary flow is maximum in $\theta = 90^\circ$ SHCHE (CR=0.14). As CR decreases, secondary flow becomes less intensive.

In addition to this, the Nu_i obtained in this study is compared with the Nu_i predicted by researchers. Correlations proposed by Mori and Nakayama [40] and Pratt [41] are selected to compare Nu_i for turbulent regimes. Also, correlation proposed by Schmidt [42, 43] is selected to compare Nu_i for the laminar regime. For all heat exchangers, when tube fluid is flowing in a laminar regime, the % variation between the Nu_i obtained in this study and the Nu_i predicted by Schmidt [42, 43] is found in the

range of 0-5%. Also, for all heat exchangers, when tube fluid is flowing in a turbulent regime, the % variation between Nu_i obtained in this study and Nu_i predicted by Pratt [41] is found in the range of 3-17%. In addition, a comparison of Nu_i predicted by Mori and Nakayama [40] with Nu_i of this study % variation is found to be in the range of 3-20 %. Thus, agreement is found between the Nu_i obtained in this study and the Nu_i predicted by researchers (Fig. 10).

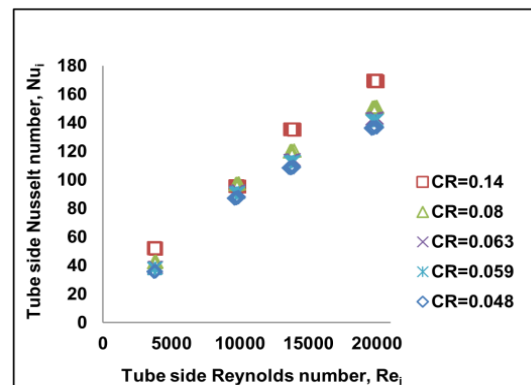


Fig. 9. Tube side Nusselt number vs. tube side Reynolds number

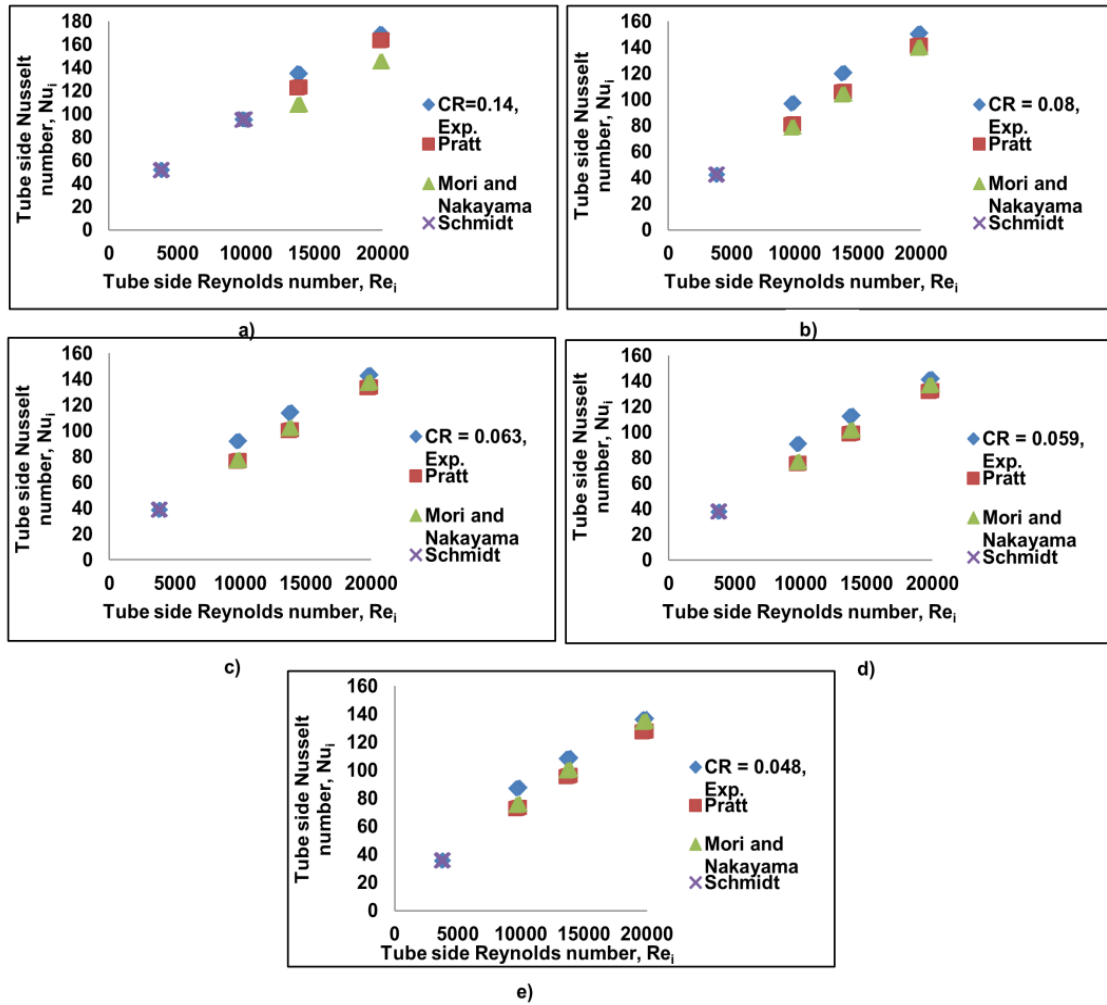


Fig. 10. Tube side Nusselt number vs. tube side Reynolds number

Also, in this study, geometry of coils is varied as SHC, CC, and spiral. Hence, it is necessary to study the shell side Nusselt number, Nu_o . Variation of Nu_o against shell side mass flow rate (m_{sc}) is plotted in Fig. 11. It is depicted that as m_{sc} increases, Nu_o increases. Maximum Nu_o is obtained for $\theta = 30^\circ$ HCCHE, and lowest Nu_o is obtained for $\theta = 90^\circ$ SHCCH. This indicates that for $\theta = 30^\circ$ HCCHE the locking of fluid between coil turns is less compared to $\theta = 90^\circ$ SHCCH. Also, when fluid flows over the turns of $\theta = 90^\circ$ SHCCH, dead zones are created in the space available between turns. In conical geometry, coil diameter is reduced in the direction of shell fluid flow, causing the flow of fluid particles over the coil to turn one by one. This causes effective contact of shell fluid with the tube surface, resulting in better heat transfer. Thus the thermal performance of $\theta = 30^\circ$ HCCHE is found to be better compared to $\theta = 90^\circ$ SHCCH, $\theta = 0^\circ$ HE, and $\theta = 70^\circ$ and 50° HCCHEs. The reasons behind this are as follows: a) for $\theta = 90^\circ$ SHC, coil diameter (D) is 0.07 m, causing the highest CR of 0.14. Keeping small end diameter equal to 0.07 m, bigger end diameters are obtained for variation in θ as 70° , 50° , 30° and 0° .

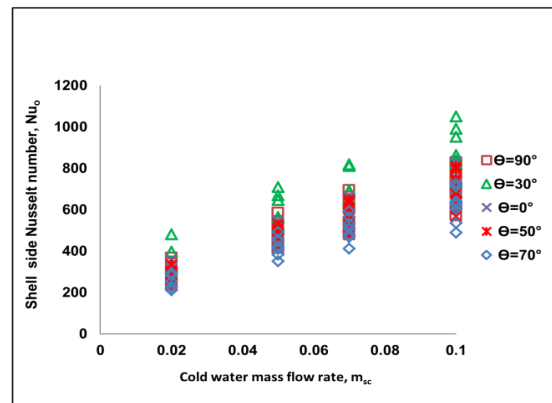


Fig. 11. Shell side Nusselt number vs. cold water mass flow rate

This resulted in a variation in CR in the range of 0.14 to 0.028. Also, HCCs are placed such that a smaller end diameter (D_c) faces the ground. Due to this, when fluid flows from a bigger diameter (CR = 0.028) to a smaller diameter (CR = 0.14), it causes an increase in secondary fluid velocities which is indicated by increased values of De_i . This assists in heat transfer. b) for $\theta = 30^\circ$ HCCHE, the position of the coil in the shell is such that the average coil diameter D_{ave} (0.21 m) is present at

the center of shell space. This makes the smaller end and bigger ends of the coil close to the inner and outer shell, respectively. This causes effective contact of cold water with the tube surface resulting in better heat transfer c) for other HCCs ($\theta=70^\circ$ and 50°), contact of shell fluid with the tube surface is comparatively higher than $\theta=90^\circ$ SHCHE. Also, due to the longest slant edge of $\theta=30^\circ$ HCCHE, better contact between shell fluid and tube surface is taking place compared to $\theta=0^\circ$ HE (spiral coil).

4.4. Pressure Drop and Friction Factor

In a coiled heat exchanger, heat transfer is increased against a rise in pressure drop. This rise in pressure drop leads to a rise in pumping power. Hence, pressure drop and pumping power are significant factors that impact the heat exchanger's design. Fig. 12 (a) and (b) depict plots of tube side pressure drop (ΔP_{ch}) vs. tube side mass flow rate (m_{ch}) for parallel flow and

counter flow, respectively. As m_{ch} rises from 0.02 to 0.1 kg/s, ΔP_{ch} rises. The highest ΔP_{ch} is obtained at $m_{ch}=0.1$ kg/s for counterflow arrangement. This is because, in a counter-flow arrangement, tube fluid is forced from the bottom against gravity. At lower values of m_{ch} , ΔP_{ch} for all heat exchangers are close to each other. But at higher values of m_{ch} (turbulent flow), maximum variation in ΔP_{ch} is found. Also, maximum ΔP_{ch} is obtained for $\theta=0^\circ$ HE and followed by $\theta=90^\circ$ SHCHE. For $m_{ch}=0.1$ kg/s and $\theta=0^\circ$ HE, ΔP_{ch} is higher by 12 % than $\theta=90^\circ$ SHCHE and by 27 % than $\theta=50^\circ$ HCCHE.

A comparison of ΔP_{ch} is done with the results of Palanisamy K et al. [19]. It is shown in Fig. 12 (c). Results are in agreement with Palanisamy K et al. [19]. Palanisamy K et al. observed higher ΔP_{ch} for HCC ($\theta=8^\circ$) in the range of 8068 -13700 Pa for water flowing in a tube having a diameter of 0.008m. For these pressure drop values, the De_i range is observed as 2200-4200.

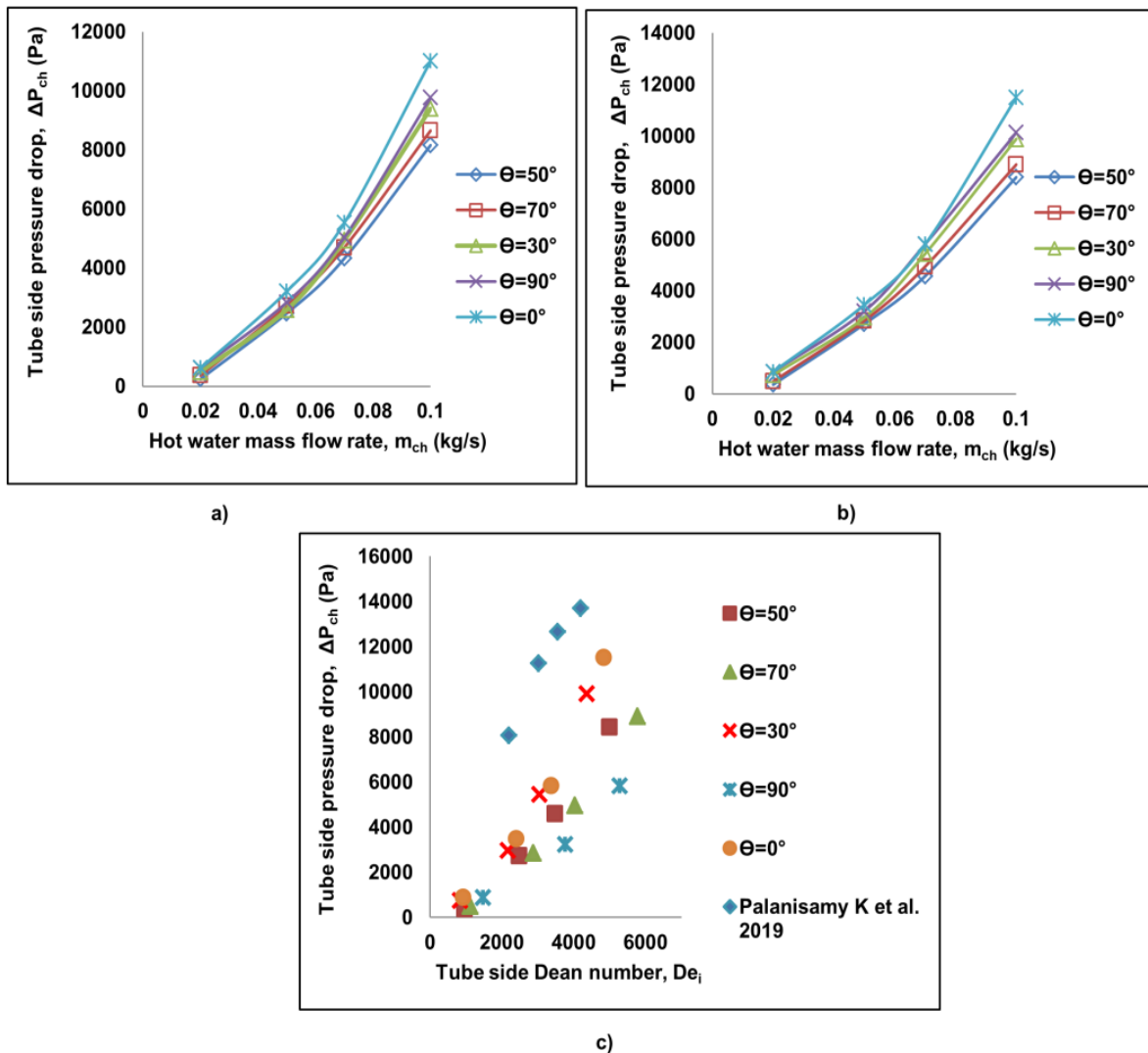


Fig. 12. Tube side pressure drop with respect to hot water mass flow rate : a) for parallel flow; b) for counter flow; c) Tube side pressure drop with respect to tube side Dean Number

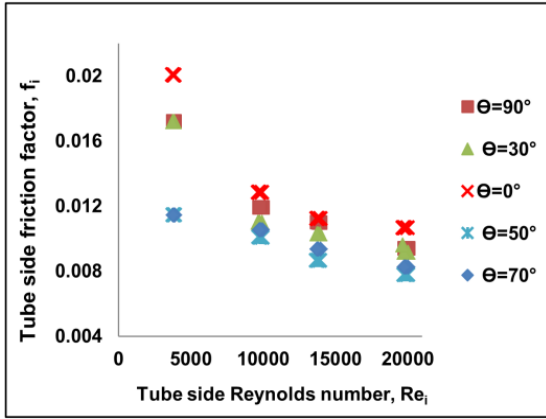


Fig. 13. Tube side friction factor vs. tube side Reynolds number

Further, ΔP_{ch} is used to calculate the tube side friction factor (f_i). Fig. 13 shows the plot of f_i versus Re_i . For all heat exchangers, as Re_i increases from laminar to turbulent regimes, f_i is found to be decreased. This is in agreement with the results of the researchers. [30, 38] Also, f_i is a function of curvature ratio (CR). When θ

increases from 50° (HCC) to 90° (SHC), the average CR increases from 0.063 to 0.14. This causes an increase in f_i . Therefore, for $\theta=90^\circ$ SHC, f_i is found to be higher than $\theta=50^\circ$ HCC. The highest f_i is obtained for $\theta=0^\circ$ HE due to its spiral shape. Purandare et al. [38] also got the highest f_i for a spiral coil compared to HCCs.

Further comparison is done between the f_i of this study and the f_i predicted by researchers. It is shown in Fig. 14. For laminar flow, the correlation proposed by Srinivasan [39] is selected. Also, turbulent flow correlations proposed by Srinivasan [44] and Mishra and Gupta are considered. [37] For almost all cases of laminar flow, the % variation in f_i is up to 20 %. Also, for turbulent flow in comparison with Srinivasan [44], the % variation in f_i is up to 20 %. Similarly, for turbulent flow in comparison with Mishra and Gupta [37], the % variation in f_i is up to 15 %. In a few cases, it has reached up to 24 %. Thus, an acceptable agreement is found between the experimental findings of this study and the researchers' predictions.

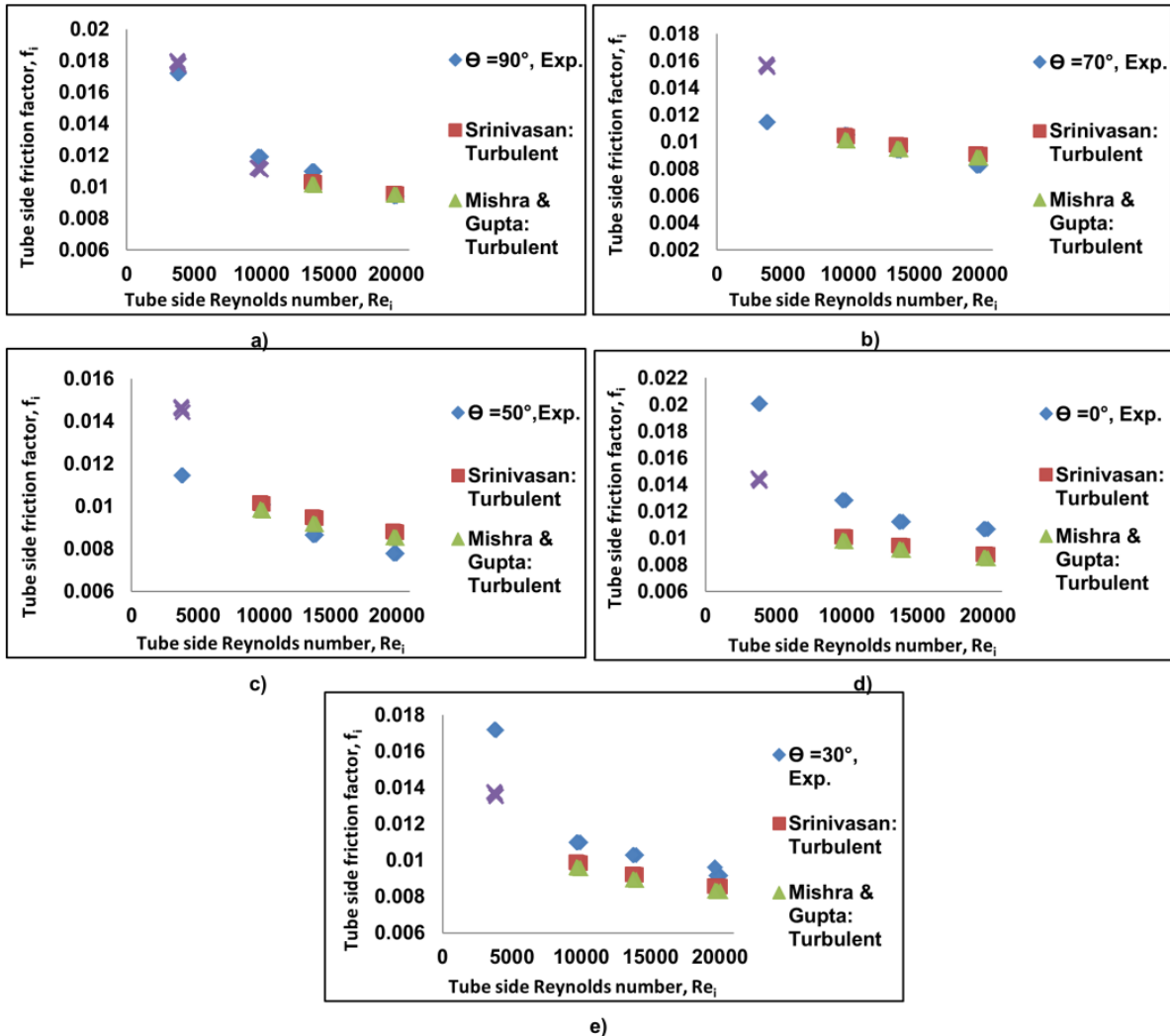


Fig. 14. Tube friction factor vs. tube side Reynolds number

In addition to ΔP_{ch} , knowledge of shell side cold water pressure drop (ΔP_{sc}) is essential as it also plays an important role in the selection of hydrodynamic parameters in the design process. In this study, cold water entry in the shell is done from the top side only. Fig.15 (a) displays a plot of ΔP_{sc} vs. m_{sc} . As m_{sc} increases from 0.02 to 0.1 kg/s, ΔP_{sc} for all heat exchangers is found to increase. At lower values of m_{sc} , ΔP_{sc} for all heat exchangers are found to be close to each other, but scatter in ΔP_{sc} values is observed at higher values of m_{sc} . For $\theta=90^\circ$ SHCHE, maximum ΔP_{sc} is found as 3091 Pa. Lowest ΔP_{sc} is found for $\theta=0^\circ$ HE. The reason behind this is the height of the shell. The height of the shell of $\theta=90^\circ$ SHCHE is the maximum, whereas the height of $\theta=0^\circ$ HE is the lowest. Also, for $\theta=30^\circ, 50^\circ$ and 70° HCCHEs, ΔP_{sc} are found close to each other.

4.5. Pumping power and pumping power per unit heat transfer area

In addition to pressure drop information about pumping power, it is very important as it is directly proportional to the cost required. For coiled tube heat exchangers, very little amount of information about pumping power and pumping power per unit heat transfer area is available in the literature. Pumping power is obtained as per Eq. (15). In the formulation, pump, or fan efficiency, η_p is considered equal to 0.80. [39] Pumping power for coil fluid is obtained, as mentioned in Table 5. It is observed that maximum PP_{ch} is required for $\theta=0^\circ$ HE because of its spiral nature. PP_{ch} is maximum for $\theta=90^\circ$ SHC compared to $\theta =70^\circ, 50^\circ$ and 30° HCC. This is because it has the highest height of 0.26 m and the lowest coil diameter ($D_{ave}=0.07m$). Similarly, the pumping power for shell cold water (PP_{sc}) is also calculated.

Table 5. Pumping power for coil fluid

Parameter	90° HE	70° HE	50° HE	0° HE	30° HE
Pumping power for hot water, $PP_{ch}(m_{ch}=0.02 \text{ kg/s})$ (W)					
Parallel flow	0.02	0.01	0.01	0.02	0.01
Counter flow	0.02	0.01	0.01	0.02	0.02
Pumping power for hot water, $PP_{ch}(m_{ch}=0.1 \text{ kg/s})$ (W)					
Parallel flow	1.23	1.09	1.03	1.33	1.19
Counter flow	1.28	1.12	1.06	1.45	1.31

The plot of PP_{sc} vs. m_{sc} is shown in Fig. 15 (b). For $\theta=0^\circ$ HE, the lowest PP_{sc} is obtained, and the maximum PP_{sc} is required for $\theta=90^\circ$ SHCHE as it has the highest height. PP_{ch} and PP_{sc} for $\theta=70^\circ,$

$50^\circ,$ and 30° HCCHE are found to be close to each other.

In addition to pumping power, pumping power per unit heat transfer area (PPUHTA) is obtained from Eq. no. 16. Table 6 lists the determined values of PPUHTA for hot water. It is observed that maximum PPUHTA for coil hot water is obtained for $\theta= 0^\circ$ HE followed by $\theta=90^\circ$ SHCHE. Additionally, they are close to each other for remaining heat exchangers.

Table 6. Pumping power per unit heat transfer area for coil fluid

Parameter	90°	70°	50°	0°	30°
Pumping power per unit heat transfer area for hot water ($m_{ch}=0.1 \text{ kg/s}$)					
Parallel flow	11.89	10.53	9.93	13.39	11.44
Counter flow	12.34	10.84	10.23	13.99	12.64
Pumping power per unit heat transfer area for hot water ($m_{ch}=0.02 \text{ kg/s}$)					
Parallel flow	0.15	0.09	0.06	0.15	0.12
Counter flow	0.21	0.12	0.09	0.21	0.18

Furthermore, PPUHTA for shell cold water is obtained for variation of m_{sc} for all heat exchangers. It is shown in Fig. 15 (c). Shell side PPUHTA for $\theta=90^\circ$ SHCHE with an equivalent diameter (D_{eq}) of 0.56 m is found as 3.12 W/m². Similarly, for $\theta=30^\circ$ HCCHE, PPUHTA is found to be 2.37 W/m² for having a D_{eq} of 0.46 m. Kakac et al. [38] discussed PPUHTA for SHCHE having a D_{eq} of 0.0241m with water ($h=3850 \text{ W/m}^2 \text{ K}$ at 27 °C). PPUHTA for this heat exchanger was given as 3.85 W/m². For comparisons, information on pumping power per unit heat transfer area for helical cone coils is not found. It is depicted that the lowest PPUHTA for shell fluid is seen for $\theta =0^\circ$ HE, whilst the highest value is seen for $\theta=90^\circ$ SHCHE. For HCCHE with $\theta=70^\circ, 50^\circ,$ and $30^\circ,$ it is discovered to be within the range. Also, for $\theta=30^\circ$ HCCHE, pressure drops, pumping power, and pumping power per unit heat transfer area for coil-side hot water and shell-side cold water are found close to heat exchangers, which have minimum values.

Thus, in this study, analysis of experimental heat transfer of coiled tubes is done on the basis of variation in curvature ratio (range= 0.14 to 0.028) and geometry (straight helical, conical, and spiral). Considering thermal and hydrodynamic performance, it is predicted that $\theta=30^\circ$ HCCHE, having an average curvature ratio of 0.048, is optimum among heat exchangers considered here.

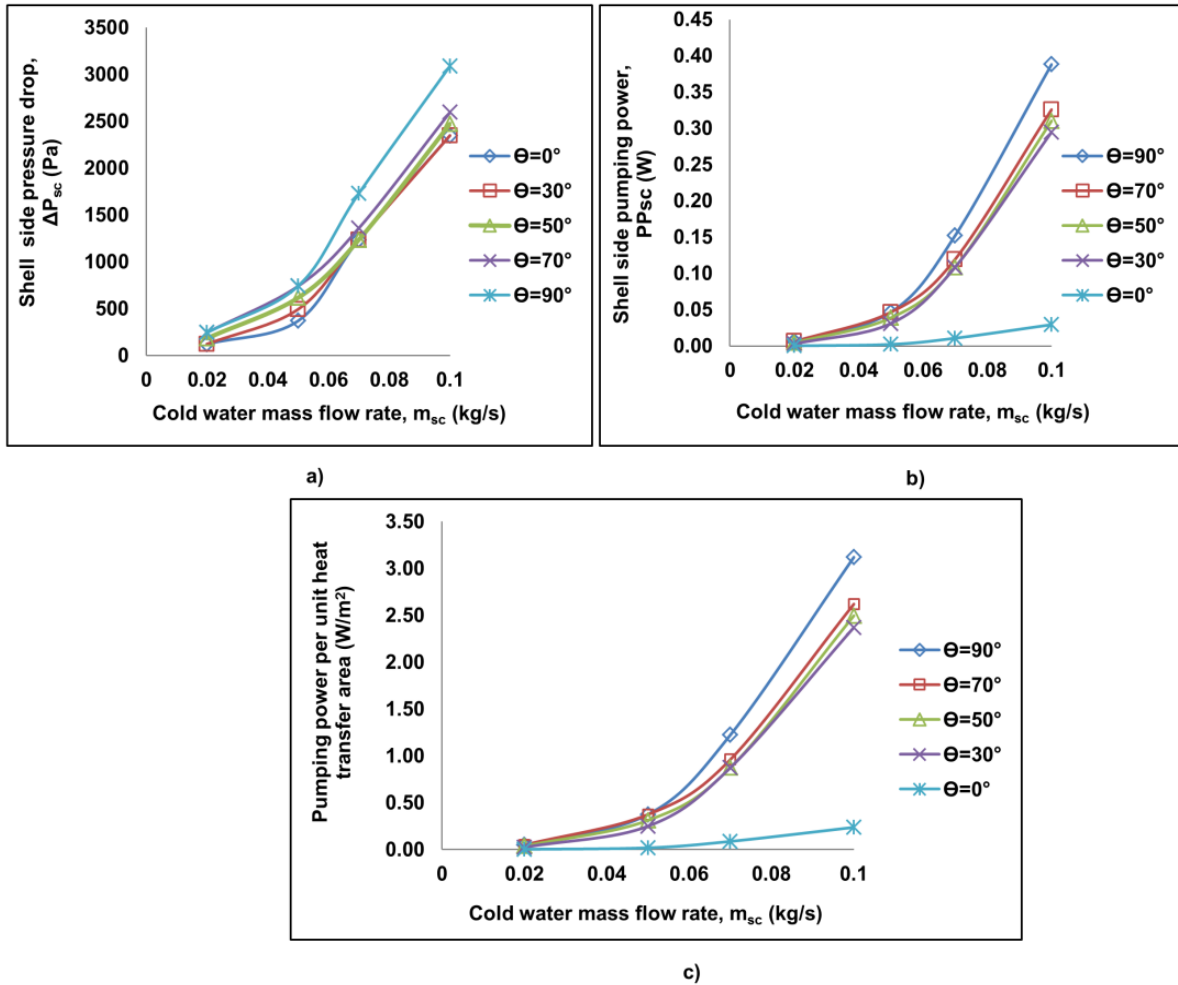


Fig. 15. Shell side cold water pressure drop, pumping power and pumping power per unit heat transfer area

5. Conclusions

In a helical cone coil (HCC), the curvature ratio increases from a bigger diameter to a smaller diameter. Also, due to conical geometry, effective contact of shell fluid occurs with the tube surface. This results in better heat transfer, but it also causes a rise in pressure drop. In order to explore this, 05 heat exchangers are manufactured keeping coil side and shell side volumes fixed, and cone angle varied between $\theta=90^\circ$ (SHC) and $\theta=0^\circ$ (spiral coil) in the steps as 70° , 50° , and 30° , for SHC coil diameter is considered equal to 0.07 m. For HCC and spiral coil, smaller coil diameter values are fixed equal to 0.07 m, and for variation of cone angle, bigger coil diameter values are obtained for constant length. This resulted in a curvature ratio range of 0.14 to 0.028. The optimum heat exchanger (HE) is predicted on the basis of thermal and hydrodynamic parameters.

- In helical cone coil heat exchanger (HCCHE), thermal and hydrodynamic properties are found better in the direction of increasing curvature ratio, causing enhancement in heat transfer. For coil hot water flow in laminar regime ($Re_i = 3700-3900$) and

turbulent regime ($Re_i = 9700-20000$), for $\theta=30^\circ$ HCC ΔT_{ch} is found to be higher by 18 % and 34 % respectively than $\theta=90^\circ$ SHC. Also, in comparison with $\theta=0^\circ$ HE, $\theta=30^\circ$ HCCHE is higher by 7 % and 24 %, respectively, for laminar and turbulent flow. Similarly, for the laminar flow regime, Q_{ch} for $\theta=30^\circ$ HCCHE is higher by 17 % than $\theta=90^\circ$ SHC and 8 % higher than $\theta=0^\circ$. Also, for turbulent flow regimes, Q_{ch} for $\theta=30^\circ$ HCCHE is higher by 23 % than $\theta=90^\circ$ SHC and 11 % than $\theta=0^\circ$ HE.

- For $\theta=30^\circ$ HCCHE, the highest effectiveness is found to be 0.61 and 0.49, respectively, for $Re_i=3854$ and $Re_i=19961$. Additionally, when compared with $\theta=90^\circ$ and 0° HEs, for $\theta=30^\circ$ HCCHE, effectiveness is higher in the range of 16 to 5 % for laminar flow and 15 to 7 % for turbulent flow. For $\theta=70^\circ$ and 50° HCCs, ΔT_{ch} , Q_{ch} , and effectiveness lie in between $\theta=90^\circ$ SHC and $\theta=0^\circ$ HE.
- For SHC, HCC, and spiral coil, modified effectiveness is found to be decreased as mass flow rate ratio increased, which is in agreement with the results of researchers.

For SHC, HCC, and spiral coil correlations are proposed for modified effectiveness, which is useful in the early stage of designing heat exchangers.

- Tube side Nusselt numbers and friction factors increase as Re_i increases, and these are found to agree with the predictions of existing researchers.
- For $\theta=0^\circ$ HE, the highest coil hot water pressure drop, ΔP_{ch} is observed and followed by $\theta=90^\circ, 30^\circ, 70^\circ,$ and 50° HEs. In addition to this, for turbulent flow and $\theta=0^\circ$ HE, ΔP_{ch} is 12 % higher than $\theta=90^\circ$ HE and 27 % higher than $\theta=50^\circ$ HE. Also, the highest shell side cold water pressure drop, ΔP_{scis} obtained for $\theta=90^\circ$ SHCHE and followed by $\theta=70^\circ, 50^\circ, 30^\circ$ and 0° HEs. Thus, for the maximum mass flow rate of shell cold water of 0.1 kg/s, ΔP_{sc} for $\theta=90^\circ$ SHCHE is 16 % higher than $\theta=70^\circ$ HE and 24 % higher than $\theta=0^\circ$ HE.
- It is observed that maximum pumping power per unit area for coil hot water is obtained for $\theta=0^\circ$ HE followed by $\theta=90^\circ$ SHCHE. Also, for $\theta=90^\circ$ SHCHE, maximum pumping power per unit heat transfer area for shell fluid is observed. For $\theta=30^\circ$ HCCHE, pumping power per unit heat transfer area for shell and coil fluids is found to be close to $\theta=70^\circ$ and 50° HCCHEs.

Therefore, on the basis of thermal and hydrodynamic parameters examined here, it is predicted that $\theta=30^\circ$ HCCHE, having an average CR of 0.048, is better than other heat exchangers studied here. For $\theta=30^\circ$ HCCHE, the conical shape of the coil causes a maximum increment in curvature ratio from base to apex and better contact of shell fluid with the coil, which results in better thermal and hydrodynamic performance.

Nomenclature

A	Area, m^2
CR	Curvature ratio
C_p	Specific heat, $J/kg^\circ K$
D	Coil diameter, m
De	Dean number
D_{eq}	Equivalent diameter, m
d	Tube diameter, m
H	Height, m
h	Hot
h	Heat transfer coefficients, $W/m^2^\circ K$
L	Coil length, m

L_{se}	Length of slant edge, m
$LMTD$	Log mean temperature Difference
m	Mass flow rate, kg/s
$(mC_p)_{min}$	Minimum Value of product of m and C_p
N	Number of turns
$Nu=h.d/k$	Nusselt number
P	Pitch, m
Pr	Prandtl Number
PP	Pumping power, W
Q	Rate of heat transfer, W
Re	Reynolds number
Re_{crit}	Critical Reynolds number
T	Temperature, $^\circ C$
t	Tube, Top
U	Overall heat transfer coefficients,
V	Volume, m^3
v	Velocity, m/s

Greek letters

ρ	Mass density, kg/m^3
μ	Dynamic viscosity, m/kgs
η_p	Pump efficiency
ϵ	Effectiveness
ϵ'	Modified effectiveness
θ	Angle, $^\circ$
ΔT	Temperature difference, $^\circ C$
ΔP	Pressure Difference, Pa

Subscripts

ave	Average
c	Cold water, Coil
bot	Bottom
top	Top
h	Hot water
i	Inner, tube side
min	Minimum
o	Outer, Outside
ov	Overall
s	Shell
si	Inner shell
so	Outer shell
t	Tube

Abbreviations

CF	Counter flow
$CTHE$	Coiled tube heat exchanger

CFD	Computational Fluid Dynamics
HCC	Helical cone coil
HCCHE	Helical cone coil heat exchanger
PF	Parallel flow
SHC	Straight helical coil
SHCHE	Straight helical coil heat exchanger

Funding Statement

This research did not receive any specific grant from funding agencies in the public, commercial, or not-for-profit sectors.

Conflicts of Interest

The author declares that there is no conflict of interest regarding the publication of this article.

References

- [1] Kakaç, S., Shah, R.K. and Aung, W., 1987. Handbook of single-phase convective heat transfer.
- [2] Prabhanjan, D.G., Raghavan, G.S.V. and Rennie, T.J., 2002. Comparison of heat transfer rates between a straight tube heat exchanger and a helically coiled heat exchanger. *International communications in heat and mass transfer*, 29(2), pp.185-191. doi: 10.1016/S0735-1933(02)00309-3
- [3] Naphon, P. and Suwagrai, J., 2007. Effect of curvature ratios on the heat transfer and flow developments in the horizontal spirally coiled tubes. *International Journal of Heat and Mass Transfer*, 50(3-4), pp.444-451. doi: 10.1016/j.ijheatmasstransfer.2006.08.002
- [4] Naphon, P., 2007. Thermal performance and pressure drop of the helical-coil heat exchangers with and without helically crimped fins. *International Communications in Heat and Mass Transfer*, 34(3), pp.321-330. doi: 10.1016/j.icheatmasstransfer.2006.11.009
- [5] Ali, M.E., 1994. Experimental investigation of natural convection from vertical helical coiled tubes. *International journal of heat and mass transfer*, 37(4), pp.665-671. doi: 10.1016/0017-9310(94)90138-4
- [6] Ghorbani, N., Taherian, H., Gorji, M. and Mirgolibabaei, H., 2010. An experimental study of thermal performance of shell-and-coil heat exchangers. *International Communications in Heat and Mass Transfer*, 37(7), pp.775-781. doi: 10.1016/j.icheatmasstransfer.2010.02.001
- [7] Ghorbani, N., Taherian, H., Gorji, M. and Mirgolibabaei, H., 2010. Experimental study of mixed convection heat transfer in vertical helically coiled tube heat exchangers. *Experimental Thermal and Fluid Science*, 34(7), pp.900-905. doi: 10.1016/j.expthermflusci.2010.02.004
- [8] Shokouhmand, H., Salimpour, M.R. and Akhavan-Behabadi, M.A., 2008. Experimental investigation of shell and coiled tube heat exchangers using Wilson plots. *International communications in heat and mass transfer*, 35(1), pp.84-92. doi: 10.1016/j.icheatmasstransfer.2007.06.001
- [9] Jayakumar, J.S., Mahajani, S.M., Mandal, J.C., Vijayan, P.K. and Bhoi, R., 2008. Experimental and CFD estimation of heat transfer in helically coiled heat exchangers. *Chemical engineering research and design*, 86(3), pp.221-232. doi: 10.1016/j.cherd.2007.10.021
- [10] Salimpour, M.R., 2008. Heat transfer characteristics of a temperature-dependent-property fluid in shell and coiled tube heat exchangers. *International Communications in Heat and Mass Transfer*, 35(9), pp.1190-1195. doi: 10.1016/j.icheatmasstransfer.2008.07.002
- [11] Kharat, R., Bhardwaj, N. and Jha, R.S., 2009. Development of heat transfer coefficient correlation for concentric helical coil heat exchanger. *International Journal of Thermal Sciences*, 48(12), pp.2300-2308. doi: 10.1016/j.ijthermalsci.2009.04.008
- [12] Moawed, M., 2011. Experimental study of forced convection from helical coiled tubes with different parameters. *Energy conversion and Management*, 52(2), pp.1150-1156. doi: 10.1016/j.enconman.2010.09.009
- [13] Ke, Y., Pei-Qi, G., Yan-Cai, S. and Hai-Tao, M., 2011. Numerical simulation on heat transfer characteristic of conical spiral tube bundle. *Applied Thermal Engineering*, 31(2-3), pp.284-292. doi: 10.1016/j.applthermaleng.2010.09.008
- [14] Elazm, A.M., Ragheb, A.M., Elsafty, A.F. and Teamah, M.A., 2011. Experimental and numerical comparison between the performance of helical cone coils and ordinary helical coils used as dehumidifier for humidification dehumidification in desalination units. *International Journal of Applied Engineering Research*, 2(1), p.104.
- [15] Flórez-Orrego, D., Arias, W., López, D. and Velásquez, H., 2012, June. Experimental and

- CFD study of a single phase cone-shaped helical coiled heat exchanger: an empirical correlation. In *Proceedings of the 25th international conference on efficiency, cost, optimization, simulation and environmental impact of energy systems* (pp. 375-394).
- [16] Kalpakli Vester, A., Örlü, R. and Alfredsson, P.H., 2016. Turbulent flows in curved pipes: Recent advances in experiments and simulations. *Applied Mechanics Reviews*, 68(5), p.050802. doi: [10.1115/1.4034135](https://doi.org/10.1115/1.4034135)
- [17] Jamshidi, N. and Mosaffa, A., 2018. Investigating the effects of geometric parameters on finned conical helical geothermal heat exchanger and its energy extraction capability. *Geothermics*, 76, pp.177-189. doi: [10.1016/j.geothermics.2018.07.007](https://doi.org/10.1016/j.geothermics.2018.07.007)
- [18] Daghigh, R. and Zandi, P., 2018. Experimental analysis of heat transfer in spiral coils using nanofluids and coil geometry change in a solar system. *Applied Thermal Engineering*, 145, pp.295-304. doi: [10.1016/j.applthermaleng.2018.09.053](https://doi.org/10.1016/j.applthermaleng.2018.09.053).
- [19] Palanisamy, K. and Kumar, P.M., 2019. Experimental investigation on convective heat transfer and pressure drop of cone helically coiled tube heat exchanger using carbon nanotubes/water nanofluids. *Heliyon*, 5(5). doi: [10.1016/j.heliyon.2019.e01705](https://doi.org/10.1016/j.heliyon.2019.e01705).
- [20] Heyhat, M.M., Jafarzad, A., Changizi, P., Asgari, H. and Valizade, M., 2020. Experimental research on the performance of nanofluid flow through conically coiled tubes. *Powder technology*, 370, pp.268-277. doi: [10.1016/j.powtec.2020.05.058](https://doi.org/10.1016/j.powtec.2020.05.058).
- [21] Ali, M., Rad, M.M., Nuhait, A., Almuzaiqer, R., Alimoradi, A. and Tlili, I., 2020. New equations for Nusselt number and friction factor of the annulus side of the conically coiled tubes in tube heat exchangers. *Applied Thermal Engineering*, 164, p.114545. doi: [10.1016/j.applthermaleng.2019.114545](https://doi.org/10.1016/j.applthermaleng.2019.114545).
- [22] Sheeba, A., Akhil, R. and Prakash, M.J., 2020. Heat transfer and flow characteristics of a conical coil heat exchanger. *International Journal of Refrigeration*, 110, pp.268-276. doi: [10.1016/j.ijrefrig.2019.10.006](https://doi.org/10.1016/j.ijrefrig.2019.10.006).
- [23] Al-Salem, K., Hosseini, E., Nohesara, A., Mehri, M., Ali, M., Almuzaiqer, R., Alimoradi, A. and Tlili, I., 2019. Suggestion of new correlations for the exergy efficiency and coefficient of exergy performance of annulus section of conically coiled tube-in-tube heat exchangers. *Chemical Engineering Research and Design*, 152, pp.309-319. doi: [10.1016/j.cherd.2019.10.002](https://doi.org/10.1016/j.cherd.2019.10.002).
- [24] Maghrabie, H.M., Attalla, M. and Mohsen, A.A., 2021. Performance of a shell and helically coiled tube heat exchanger with variable inclination angle: experimental study and sensitivity analysis. *International Journal of Thermal Sciences*, 164, p.106869. doi: [10.1016/j.ijthermalsci.2021.106869](https://doi.org/10.1016/j.ijthermalsci.2021.106869)
- [25] Chokphoemphun, S., Eiamsa-ard, S., Promvong, P., Thongdaeng, S. and Hongkong, S., 2021. Heat transfer of a coil-tube heat exchanger in the freeboard zone of a rice husk fluidized-bed combustor. *International Communications in Heat and Mass Transfer*, 127, p.105462. doi: [10.1016/j.icheatmasstransfer.2021.105462](https://doi.org/10.1016/j.icheatmasstransfer.2021.105462)
- [26] Hassaan, A.M. and Mostafa, H.M., 2021. Experimental study for convection heat transfer from helical coils with the same outer surface area and different coil geometry. *Journal of Thermal Science and Engineering Applications*, 13(5), p.051012. doi: [10.1115/1.4049870](https://doi.org/10.1115/1.4049870)
- [27] Hassaan, A.M., 2022. An Experimental Investigation for the Use of Multi-Wall Carbon Nanotubes Based on Water Nanofluid in a Plate Heat Exchanger. *Heat Transfer Research*, 53(16). doi: [10.1615/HeatTransRes.2022042147](https://doi.org/10.1615/HeatTransRes.2022042147)
- [28] Hassaan, A.M., 2023. Experimental investigation of the performance of the plate heat exchanger using (Multi-Walled Carbon Nanotubes-Al₂O₃/water) hybrid nanofluid. *Proceedings of the Institution of Mechanical Engineers, Part E: Journal of Process Mechanical Engineering*, 237(4), pp.1310-1318. doi: [10.1177/09544089221113977](https://doi.org/10.1177/09544089221113977)
- [29] Sharma, S., Sah, A., Subramaniam, C. and Saha, S.K., 2021. Performance enhancement of tapered helical coil receiver using novel nanostructured carbon florets coating. *Applied Thermal Engineering*, 194, p.117065. doi: [10.1016/j.applthermaleng.2021.117065](https://doi.org/10.1016/j.applthermaleng.2021.117065)
- [30] Hassaan, A.M., 2022. An investigation for the performance of the using of nanofluids in shell and tube heat exchanger. *International Journal of Thermal Sciences*, 177, p.107569. doi: [10.1016/j.ijthermalsci.2022.107569](https://doi.org/10.1016/j.ijthermalsci.2022.107569)
- [31] Hassaan, A.M., 2022. Evaluation for the performance of heat transfer process in a double pipe heat exchanger using nanofluids. *Proceedings of the Institution of Mechanical Engineers, Part E: Journal of Process Mechanical Engineering*, 236(5),

- pp.2139-2146.
[doi: 10.1177/09544089221086825](https://doi.org/10.1177/09544089221086825)
- [32] Hassaan, A.M., 2023. Comparing the performance of using nanofluids in two different types of heat exchangers with the same heat transfer area. *Heat Transfer Research*, 54(18). doi: 10.1615/HeatTransRes.2023045768
- [33] Omri, M., Aich, W., Rmili, H. and Kolsi, L., 2022. Experimental Analysis of the Thermal Performance Enhancement of a Vertical Helical Coil Heat Exchanger Using Copper Oxide-Graphene (80-20%) Hybrid Nanofluid. *Applied Sciences*, 12(22), p.11614. doi: 10.3390/app122211614.
- [34] Alklaibi, A.M., Mouli, K.V.C. and Sundar, L.S., 2023. Experimental investigation of heat transfer and effectiveness of employing water and ethylene glycol mixture based Fe₃O₄ nanofluid in a shell and helical coil heat exchanger. *Thermal Science and Engineering Progress*, 40, p.101739. doi: org/10.1016/j.tsep.2023.101739
- [35] Abdullah, M.S. and Hussein, A.M., 2023. Thermal Performance of a Helical Coil Heat Exchanger Utilizing Nanofluids: A Review. *Journal of Heat and Mass Transfer Research*, 10, pp.121-134. doi: 10.22075/jhmtr.2023.30124.1428
- [36] Kline, S.J., 1963. Describing uncertainties in single-sample experiments. *Mech. Eng.*, 75, pp.3-8.
- [37] VDI Society for Porous Engineering and Chemical, 2010. *VDI heat atlas*. Verlag Berlin
- Heidelberg: Springer. doi: 10.1007/978-3-540-77877-6_36
- [38] Purandare, P.S., Lele, M.M. and Gupta, R.K., 2015. Investigation on thermal analysis of conical coil heat exchanger. *International Journal of Heat and Mass Transfer*, 90, pp.1188-1196. doi: 10.1016/j.ijheatmasstransfer.2015.07.044
- [39] Kakaç, S., Liu, H. and Pramuanjaroenkij, A., 2002. *Heat exchangers: selection, rating, and thermal design*. CRC press.
- [40] Sigalotti, L.D.G., Alvarado-Rodríguez, C.E. and Rendón, O., 2023. Fluid Flow in Helically Coiled Pipes. *Fluids*, 8(12), p.308. doi: 10.3390/fluids8120308
- [41] Mori, Y. and Nakayama, W., 1967. Study of forced convective heat transfer in curved pipes (2nd report, turbulent region). *International journal of heat and mass transfer*, 10(1), pp.37-59. doi: 10.1016/0017-9310(67)90182-2
- [42] Sobota, T., 2011. Experimental prediction of heat transfer correlations in heat exchangers. *Developments in Heat Transfer*, pp.294-308. doi: 10.5772/20362
- [43] Smith, E.M., 2005. *Advances in thermal design of heat exchangers*. Wiley. doi: 10.1002/0470017090
- [44] Sun, S., Liu, J., Sang, R. and Zhao, K., 2022. Experimental study of flow friction behavior in coiled tubing. *Energy Reports*, 8, pp.187-196. doi: 10.1016/j.egy.2022.10.291